doi.org/10.36721/PJPS.2026.39.4.REG.13812.1

Ethnic medicine *Bauhinia brachycarpa* Benth regulates microglia-neuron interaction in neuropathic pain via P2X4R-BDNF-TrkB pathway

Han-Fu Liu[1], Ya-Nan Chen[1], He Sun[1], Bei Jiang[1,2], Jin-Da Wang[2*] and Lei Shen[1,2*]

[1]Yunnan Key Laboratory of Screening and Research on Anti-Pathogenic Plant Resources from Western Yunnan, Dali, People's Republic of China

[2]College of Pharmacy, Dali University, Dali, People's Republic of China

Abstract: **Background**: Neuropathic pain (NP) is a debilitating condition with limited treatment options. The ethanolic extract of Bauhinia *brachycarpa Benth* (EEBb) has demonstrated antinociceptive effects in NP, but its active components and underlying mechanisms of action remain largely unexplored. **Objectives**: Bauhinia brachycarpa Benth (BBB), an ethnic medicine in China, has antinociceptive effect on neuropathic pain (NP). In this study, an effective portion from BBB was screened and its antinociceptive mechanism was investigated. **Methods**: After the preparation of ethanolic extract from BBB (EEBb) and different soluble portion from EEBb (peEEBb, eaEEBb, nbEEBb), the total content of flavonoids and phenolic acids were measured. A partial sciatic nerve ligation (PSNL) model in vivo was applied to evaluate the antinociceptive effect and the influence on microglia function of these samples. The possible acting target of BBB was predicted by network pharmacology. And the mechanism of nbEEBb, the most effective antinociceptive portion, were studied by PSNL model in vivo and ATP-induced activation of BV2 model in vitro. **Results**: nbEEBb had the strongest ability of alleviating NP as well as the obvious effect on microglia polarization. The action of nbEEBb was positively correlated to the total content of flavonoids or phenolic acids. nbEEBb inhibited the protein and gene expressions of most key components in P2X4-BDNF-TrkB signaling pathway. **Conclusion**: nbEEBb is the most effective portion from BBB on NP, and its mechanism refers to the inhibition of P2X4-BDNF-TrkB signaling pathway, which involved in neuron-microglia interaction.

Keywords: *Bauhinia brachycarpa* Benth; Microglia-neuron interaction; Neuropathic pain; P2X4R-BDNF-TrkB signaling pathway

Submitted on 06-12-2024 – Revised on 09-10-2025 – Accepted on 11-10-2025

INTRODUCTION

The function of somatosensory system is to perceive pressure, touch, temperature, movement, position and vibration. Neuropathic pain (NP), characterized by hyperalgesia, allodynia and spontaneous pain, is a distinct type of pain resulting from lesions or dysfunctions in the somatosensory system. (Colloca L *et al*., 2017; Bannister K *et al*., 2020). Currently, drug therapy is the primary approach for managing NP, but clinical challenges such as limited efficacy, frequent adverse effects and significant individual variability remain prevalent. (Kaye AD *et al*., 2025). The refractory nature of NP, especially in its later stages, is largely attributed to hyperalgesia states induced by non-neuronal cells like microglia and macrophages (Li XL *et al*., 2021; Wang LJ *et al*., 2020). However, current medications for NP, such as anticonvulsants, tricyclic antidepressants and selective 5-HT reuptake inhibitors, primarily target excessive neuronal firing without addressing the involvement of non-neuronal cells (Kaye AD *et al*., 2025). Therefore, the search for effective therapies targeting non-neuronal cells to treat NP remains necessary. Both central and peripheral sensitization are fundamental for the development of NP. Microglia, the immunocompetent cells of the central nervous system, is an essential component of central sensitization in NP and participates in every stage of the mechanisms driving this chronic pain (Karavis MY *et al*., 2023). These cells are distributed at every synapse throughout the somatosensory pathway. Persistent microglial activation following acute nerve injury or chronic dysfunction leads to the upregulation of microglia-specific molecules, including cell surface receptors and intracellular proteins. This process promotes the release of signaling molecules such as neurotrophins and inflammatory mediators, facilitating the transmission of nociceptive signals to the cerebral cortex. (Sun C *et al*., 2023; Echeverria VM *et al*., 2024). These alterations generate and maintain a maladaptive state in which neuronal overactivity produces pain intermittently, even without the original painful stimuli. Thus, studying microglia-neuron interactions is pivotal for NP treatment.

Traditional therapies like acupuncture and ethnomedicine offer attractive advantages, including broad applicability, low cost and fewer adverse effects. Thus, these treatments are suitable for certain chronic and intractable diseases, including NP (Li SH *et al*., 2020; Hu N *et al*., 2024). *Bauhinia brachycarpa* Benth (BBB, full name is *Bauhinia*

**Corresponding author:* e-mail: shenlei@dali.edu.cn; wangjinda1982@126.com

brachycarpa Wall. ex Benth. (*var brachycarpa*)) is a species within the *Bauhinia* genus of Leguminosae, widely distributed across China, particularly in Yunnan province (Flora of China, 1980). For centuries, BBB has been utilized as a traditional folk medicine among Yunnan's Han, Bai and Yi communities, documented in their medicinal records under the local names 'Ye-Guang-Men', 'Gui-Ding-Ba' and 'Pi-Mi-Li', respectively (Jiang B and Xiao CJ, 2021; Yi Medicine Records, 1983). The primary indications for BBB extract include its tranquilizing and analgesic properties, such as in the treatment of neurosis, myalgia and bone pain. Recently, we studied the antinociceptive effect of ethanolic extract from BBB (EEBb) to validate its traditional application. Results demonstrated that EEBb alleviated NP in models of trigeminal neuralgia and sciatic neuropathy. (Chen YN *et al*., 2022a; Chen YN *et al*., 2022b). The antinociceptive effects of EEBb on NP were associated with its anti-inflammatory properties. Moreover, 13 compounds have been isolated from BBB, including 8 flavonoids (such as luteolin, quercetin and (-)-epicatechin), 3 triterpenoids (such as β-sitosterol) and 2 sterols (such as daucosterol). (Shan H, 2017). However, the antinociceptive mechanisms of BBB and its associated active constituents remain unclear.

Taken together, this study aims to screen the most effective fraction of BBB on NP and elucidate whether its acting mechanism is related to central pain sensitization induced by microglia.

MATERIALS AND METHODS

Preparation of EEBb as well as the fraction extracted from EEBb

The aerial parts of BBB were collected from Dali City, Yunnan Province, China and authenticated morphologically by Dr. De-Quan Zhang from Dali University's College of Pharmacy. A voucher specimen was deposited at the Yunnan Key Laboratory of Screening and Research on Anti-pathogenic Plant Resources from Western Yunnan, Dali University (plant sample preservation number: 20190722-1). Dried twigs and leaves of BBB (19.5 kg) were powdered and extracted five times with 95% ethanol (each extraction lasting 24 hours). The extract was then concentrated and lyophilized. The resulting freeze-dried powder of EEBb was dispersed in water and subjected to sequentially polarity-based fractionated using immiscible organic solvents (petroleum ether → EtOAc → n-BuOH) in ascending order of polarity. This process yielded the petroleum ether-soluble fraction (peEEBb, 29.96 g), the ethyl acetate-soluble fraction (eaEEBb, 4.75 g) and the n-butanol-soluble fraction (nbEEBb, 75.88 g).

Chemicals and reagents

Catgut (Lot No. 24X0308J) was purchased from Jinhuan Medical Co. Ltd (Shanghai, China). Pregabalin (PGB, Lot No. DA4519) was procured from Pfizer Inc (USA). The cell culture medium, Dulbecco's Modified Eagle Medium (DMEM) and fetal bovine serum (FBS) were products of Gibco (USA). Bovine serum albumin (BSA, Lot No. 1016J051) was supplied by Solarbio (Beijing, China). Adenosine triphosphate (ATP, Lot No. 102491345) was provided by Sigma (USA). CCK-8 assay kits (Lot No. 21315903) were purchased from Biosharp Biotechnologies (Anhui, China). ELISA assay kits were obtained from Enzyme-linked Biotechnology (Shanghai, China). Drug formulations were prepared using a 0.5% CMC-Na solution (for *in vivo* applications) or DMEM supplemented with 0.2% BSA (for *in vitro* applications).

Quantification of total content of flavonoids and phenolic acids

The total flavonoid content was measured using aluminum nitrate [$Al(NO_3)_3$] colorimetry. Briefly, 1 mL of the sample solution (EEBb or its soluble fractions were diluted in methanol to a concentration of 1.6 mg/mL) was transferred to a 25 mL volumetric flask. Sequentially, 1 mL of 5% $NaNO_2$, 1 mL of 10% $Al(NO_3)_3$ and 10 mL of 4% NaOH were added to the flask, followed by distilled water to bring the total volume to 25 mL. The mixture was then set aside for 15 minutes. Simultaneously, rutin methanolic solutions with concentrations ranging from 0.008 to 0.048 mg/mL were prepared as standards. Absorbance at 508 nm was measured using a spectrophotometer (Persee General Instrument Co. Ltd, Beijing, China) following sample preparation. The total flavonoid content was calculated using a rutin-based calibration curve established through external standard calibration, with results expressed as rutin per gram of EEBb or its respective fractions. (Gong M *et al*., 2019).

The total phenolic acid content was quantified using Prussian blue colorimetry. Briefly, a 1 mL sample solution (EEBb or different soluble extract fractions from EEBb diluted in 70% ethanol at a concentration of 0.2 mg/mL) was transferred to a 25 mL brown volumetric flask. Subsequently, 2 mL of 0.3% sodium dodecyl sulfate, 1 mL mixed solution of 0.6% $FeCl_3$ and $K_3[Fe(CN)_6]$ (1:1 v/v) and 4 mL absolute ethanol were added sequentially to the flask. The mixture was allowed to react in the dark for 5 minutes. To complete the procedure, 0.1 mol/L HCl was supplemented to adjust the final volume to 25 mL, after which the solution remained in the dark for 20 minutes. At the same time, caffeic acid standard solutions (0.0008-0.0048 mg/mL) were prepared in 70% ethanol. Spectrophotometric readings at 728 nm were recorded after sample preparation. A caffeic acid standard solution was used to generate a calibration curve for quantifying total phenolic acid content in the samples. Results were reported in g of caffeic acid / g of EEBb or per each extract fraction. (Zhang Y *et al*., 2018)

Animals and treatments

Male *C57BL/6* mice (SPF-grade, 6-8 weeks) were

purchased from Beijing Speifu Biotechnology Co. Ltd. The mice were housed in a controlled environment with a 12-hour light/dark cycle at 20±3°C and given free access to food and water.

To assess the effects of the extract fraction from EEBb on sciatica, mice were randomly assigned to eleven groups as follows: Sham operation group, PSNL model group, positive drug PGB group (60 mg/kg), high dose (1000 mg/kg) and low dose (500 mg/kg) of EEBb, peEEBb, eaEEBb and nbEEBb groups. All dosages mentioned above have been proved effective in the pre-experiments. The sciatic nerve of mouse in sham group was only exposed without ligation, while the other groups underwent nerve ligation to induce injury. From day 4 to 10 post-surgery, drug-treated mice received daily medications (0.2 mL/ 10 g) while sham and model groups were administered 0.5% CMC-Na vehicle.

To investigate the mechanism of nbEEBb *in vivo*, mice were randomly assigned to five groups as follows: normal group, normal + nbEEBb group, sham operation group, PSNL model group and PSNL + nbEEBb treatment group. Then, the mice in the normal and normal + nbEEBb groups did not undergo any surgical procedures throughout the study. The mice in the sham, PSNL model and PSNL + nbEEBb groups underwent identical surgical procedures as described earlier. Following surgery or at the corresponding time points, the normal + nbEEBb and PSNL + nbEEBb groups were administered 1000 mg/kg nbEEBb daily (0.2 mL/ 10 g, days 4-10). The normal, sham and model groups got 0.5% CMC-Na vehicle.

NP model establishment and nociceptive behavior assessment

Peripheral NP was induced using the PSNL model. In detail, mice were anesthetized via intraperitoneal injection of sodium pentobarbital at 50 mg/kg. Under an anesthesia condition, the left sciatic nerve was exposed by an incision and one-third to one-half of the sciatic nerve was ligated with an 8-0 catgut suture. Wound closure was achieved with absorbable sutures, followed by iodophor antisepsis. (Chen YN *et al*., 2022b).

Paw withdrawal mechanical threshold (PWMT) was assessed as follows: Each mouse was randomly placed in one transparent box on an elevated wire mesh platform for a 1-hour acclimation period. Von Frey filaments, ranging from 0.008 g to 2 g were applied perpendicularly to the plantar surface of the mice's left hind paw by one experimenter that was ignorant of experiment design. Each stimulus was maintained for 4-6 seconds. A positive response was characterized by paw lifting and licking. The instantaneous stiffness value was captured and logged. During each testing session, animals were subjected to ten sequential stimulations administered at 1-min intervals. The test was concluded once at least seven positive responses were elicited, with the mean value of these responses calculated as the PWMT. Data analysis was subsequently performed by experiment designer. PWMT was measured on day 1 pre-operation and on days 3, 7 and 10 post-operation or corresponding time. (Chen YN *et al*., 2022b).

Cells and treatments

BV2 microglia cells were obtained from Procell Life Science and Technology Co. Ltd. (Wuhan, China) and cultured in high-glucose DMEM supplemented with 10% FBS in a CO_2 incubator (5% CO_2, 37°C). To investigate the mechanism of nbEEBb *in vitro*, cells were seeded into a 96-wells culture plate and divided into four groups: normal group, normal + nbEEBb group, model group, model + nbEEBb group. Posterior to 24 h cultivation, the medium was substituted by the vehicle (DMEM containing 0.2% BSA) or drug solution (vehicle + 0.3 mg/mL nbEEBb) for 12 h incubation. Then, 50 μM ATP was added to replace the media in the model or model + nbEEBb group for 1 h to induce BDNF release, while vehicle was given to substitute the media in the normal or normal + nbEEBb group. (Gard A *et al*., 2023).

Sample collection

In vivo, following the final PWMT measurement, blood samples were collected from mice via the posterior venous plexus and serum was prepared by centrifugation (HC-3018R, Anhui Zhongke Zhongjia Scientific Instrument Co., China) at 3000 rpm for 10 min. Upon completion of the experiment and post-euthanasia, the relevant lumbar spinal cord segments (L4-L6) were harvested as tissue samples. *In vitro*, after treatments with ATP or vehicle, the cells and supernatants of culture media were collected as samples, respectively. (Chen YN *et al*., 2022b).

Enzyme-linked immunosorbent assay (ELISA)

BDNF concentration was measured by ELISA.

qRT-PCR analysis

RNA-easy^{TM} isolation reagent (Vazyme Biotech Co., Ltd, Nanjing, China) was used to extract the total RNA from the samples. The first strand cDNA was synthesized using the All-in-one RT SuperMix Perfect for qPCR kit (Vazyme Biotech Co., Ltd). qRT-PCR analysis was conducted with ChamQ Universal SYBR qPCR Master Mix (Vazyme Biotech Co., Ltd) on a Real-Time PCR Detection System (CFX96, Bio-Rad Laboratories, USA). The primers for cDNA sequences were designed by Shanghai Sheng-Gong Bioengineering Technology Service Co., Ltd. and were presented in table 1. Gene expression levels were normalized to GAPDH mRNA expression and calculated using the $2^{-\geq\geq Ct}$ method. Each sample was measured twice in parallel and the mean was used as the relative gene expression of the sample (Chen YN *et al*., 2022b; Gard A *et al*., 2023).

Table 1: Primer sequences for qRT-PCR.

Gene	Sense (5'- 3')	Antisense (5'- 3')
	In spinal cord tissue	
Iba-1	GACGTTCAGCTACTCTGACTTT	GTTGGCCTCTTGTGTTCTTTG
CD16	TGGACACGGGCCTTTATTTC	GAGCCTGGTGCTTTCTGATT
CD206	TCAGCTATTGGACGCGAGGCA	TCCGGGTTGCAAGTTGCCGT
P2X4R	ATCGTCACCGTGAACCAGAC	GCGTCTGAATCGCAAATGCT
BDNF	GGTCACAGCGGCAGATAAAAAG	TTCGGCATTGCGAGTTCCAG
TrkB	ACTGGACCACGCCAACTGAC	TCACCACCACGGCATAGACC
GAPDH	GTGTTTCCTCGTCCCGTAGA	AATCTCCACTTTGCCACTGC
	In BV2 cell	
P2X4R	ATCGTCACCGTGAACCAGAC	GCGTCTGAATCGCAAATGCT
BDNF	TGCAGGGGCATAGACAAAAGG	CTTATGAATCGCCAGCCAATTCTC
GAPDH	AGGTCGGTGTGAACGGATTTG	GGGGTCGTTGATGGCAACA

Western blot analysis

The samples (tissue or BV2 cells) were lysed using RIPA buffer (Solarbio, Beijing, China) and protein concentrations were quantified with a BCA kit (Solarbio, Beijing, China). Proteins were isolated by SDS-PAGE and transferred onto a polyvinylidene fluoride (PVDF) membrane. Following blocking with 5% skimmed milk, the membrane was incubated overnight at 4°C with primary antibody (rabbit anti-mouse IgG) against Iba-1 (1:2000, Abcam, UK), CD16 (1:1000, Abcam, UK), CD206 (1:1000, Cell Signaling Technology, USA), P2X4R (1:1000, Santa cruz biotechnology, USA), BDNF (1:1000, Abcam, UK), p38 (1:1000, Cell Signaling Technology, USA), p-p38 (1:1000, Cell Signaling Technology, USA), TrkB (1:1000, Abcam, UK), p-TrkB (1:1000, Abcam, UK) and GAPDH (1:1000, Cell Signaling Technology, USA). Subsequently, the membrane was incubated for 1 hour with a peroxidase-conjugated secondary antibody (goat anti-rabbit IgG, Zhongshan Jinqiao, Beijing, China). Protein bands were analyzed using a gel imaging system (GBOX, Gene, UK) and expression levels were normalized to GAPDH. (Chen YN *et al*., 2022b; Davis M *et al*., 2024).

Network pharmacology

After collecting the reported compounds in BBB, active compounds were screened based on their pharmacokinetics (good gastrointestinal absorption) and druggability (comply at least three standards of druggability in total five) of the monomers with the help of SwissADME database (http://www.swissadme.ch). The potential targets of these screened compounds were then predicted through the SwissTargetPrediction database (http://www.swisstargetprediction.ch). To find disease targets, the keyword "neuropathic pain" or "inflammation" were used to search within disease database (GeneCards, https://www.genecards.org and OMIM, http://www.omim.org). The overlapping targets were regarded as inflammation targets in NP. Then, the potential target genes of BBB and the disease target genes were analyzed using the online bioinformatics platform (http://www.bioinformatics.com.cn) to obtain the overlapping targets, which were applied as the potential therapeutic targets of BBB for neuroinflammation. These overlapping target genes were imported into the STRING database (the search species is limited to "mus musculus") to determine potential protein interactions with protein–protein interaction (PPI) scores > 0.4. Cytoscape 3.9.1 was used to visualize the PPI network, construct the "compound-target-disease" network and obtain the potential core targets according to the degree algorithm. The Metascape database (https://metascape/org/gp) was applied to conduct Gene Ontology (GO) or Kyoto Encyclopedia of Genes and Genomes (KEGG) enrichment analyses, which evaluated target genes at the biological functional level or their related key signaling pathways, respectively.

Statistical analysis

Statistical analysis was performed using SPSS 20.0 software. Data were described as average ± standard deviation. One-way analysis of variance (ANOVA) followed by the Tukey´s *post hoc* test was employed to study the differences between groups. The $P < 0.05$ is regarded to be statistically significant. The correlation between PWMT and the content of active substance was analyzed by *Pearson* method with GraphPad Prism 8.0.2 software.

RESULTS

nbEEBb has the strongest ability of reducing mechanical hyperalgesia after PSNL in mice. Its antinociceptive effects are associated with flavonoid and phenolic acid content

Exposure of the sciatic nerve without ligation slightly decreased PWMT of mice in the sham group after surgery. In comparison with the sham, the nerve injury induced by ligation produced a significant reduction of PWMT in 3 days after operation that was observed in the model (PSNL + vehicle) and drug treatment (PSNL + drug) groups (Fig. 1A). All the treatments with different drugs had the ability to increase PWMT. In comparison with the model group on the 10th day, the PWMT values were significantly increased in 60 mg/kg PGB, 1000 mg/kg of EEBb, eaEEBb

and nbEEBb groups ($P < 0.01$) (Fig. 1A). The inhibitory effects of fractions with the dose of 1000 mg/kg on mechanical hyperalgesia were nbEEBb > eaEEBb > peEEBb.

To explore the potentially antinociceptive substances in EEBb, the contents of 2 active substances (flavonoids and phenolic acids) related to NP were measured and the correlations between the content of these substances and PWMT were evaluated. Quantitative colorimetric analysis showed the total content of flavonoids in the samples of EEBb, peEEBb, eaEEBb and nbEEBb was 0.583 ± 0.052, 0.400 ± 0.037, 0.678 ± 0.043 and 0.911 ± 0.030 g rutin/ g, respectively and the total content of phenolic acids in which above was 0.181 ± 0.010, 0.108 ± 0.008, 0.238 ± 0.017 and 0.305 ± 0.012 g caffeic acid/ g, respectively (Fig. 1B). Therefore, the calculated correlation coefficient (*Pearson* value) in the relationship of PWMT (10^{th} day after operation) *vs.* flavonoids content and PWMT (10^{th} day after operation) *vs.* phenolic acids content was 0.978 and 0.942, respectively (Fig. 1C). The results indicated that the content of total flavonoids or total phenolic acids had a positive correlation with antinociceptive effect produced by these extracts.

nbEEBb has the obvious effect of regulating microglia polarization

Microglia polarization is involved in central pain sensitization of NP via its two major subtypes, that is, the pro-inflammatory M1 phenotype and the anti-inflammatory M2 phenotype. To explore the effects of EEBb and different extract fractions from EEBb on microglia polarization, ionized calcium-binding adapter molecule 1 (Iba-1), CD16 and CD206 were used as the marker for total microglia, the M1 subtype and M2 subtype, respectively. Western blot analysis demonstrated that, compared to sham control, PSNL significantly increased Iba-1 and CD16 protein expressions with little action on CD206 expression (Fig. 2A). After drug treatment, high dose and low dose of EEBb and nbEEBb as well as low dose of eaEEBb significantly reduced Iba-1 protein levels ($P < 0.01$ or $P < 0.05$ vs. model). All drugs except PGB and 500 mg/kg eaEEBb markedly attenuated CD16 expression ($P < 0.01$ or $P < 0.05$). However, only EEBb and nbEEBb (1000 mg/kg) enhanced CD206 protein expression ($P < 0.05$). (Fig. 2A).

At the transcriptional level, qRT-PCR analysis revealed consistent trends: All treatments obviously downregulated Iba-1 mRNA expression ($P < 0.01$ vs. model), while most treatments except 500 mg/kg EEBb and 1000 mg/kg peEEBb significantly reduced CD16 mRNA expression ($P < 0.01$). Unlike the influence on protein expression, all drugs except PGB and EEBb remarkably upregulated CD206 mRNA expression ($P < 0.01$ or $P < 0.05$ vs. model). (Fig. 2B). Noteworthily, only nbEEBb could modulate both protein and mRNA levels of all three biomarkers.

Network pharmacology prediction

For further exploration of BBB acting mechanism on NP, network pharmacology analysis was applied. The analysis was limited to inflammation associated pathway in NP since the obvious effect of EEBb on inflammation. In virtue of databases, 8 qualified active components in the BBB were obtained and 89 potential targets genes related to these compounds were predicted. Then, 1396 overlapping diseases targets between NP and inflammation were screened. After removing duplicate targets, 42 crossover targets between compounds and disease were identified by Venn diagram (Fig. 3A). The detailed information of the 8 qualified active components and the 42 crossover targets is provided in Supplementary Table 1 and Supplementary Table 2, respectively. The PPI network of compound-disease targets, constructed using the STRING database, comprised 42 nodes and 223 edges with an average node degree of 10.6. According to the topology analysis, the 10 core target genes were *AKT1*, *MAPK3*, *GSK3B*, *MAPK14*, *PPARG*, *HSP90AA1*, *MTOR*, *PTGS2*, *F2* and *BRAF* (Fig. 3B). Importantly, several of these core targets are key downstream effectors within the BDNF-TrkB signaling pathway, which is central to neuroplasticity and pain modulation in NP. Specifically, *AKT1*, *MTOR*, *GSK3B* and *MAPK3* (*ERK1*) are well-established critical mediators directly activated upon TrkB receptor binding by BDNF, linking BBB's potential actions to this pivotal pathway. Then, a “compound-target-disease” network graph was constructed through Cytoscape software. The graph had 109 nodes and 398 edges and contained 8 compounds, 1 disease and 89 targets (Fig. 3C).

Based on the Gene Ontology (GO) enrichment analysis, 30 target genes, whose degree value was greater than the average, were enriched in 620 biological processes (BP), 41 cell compositions (CC) and 37 molecular functions (MF). The top ten terms in each category are presented in Fig. 3D. The top BP were positive regulation of protein phosphorylation, response to peptide and response to hormone. The top MF were protein kinase activity, phosphotransferase activity, alcohol group as acceptor and kinase activity. Based on the Kyoto Encyclopedia of Genes and Genomes (KEGG) enrichment analysis, 30 target genes were enriched in 140 signaling pathways and the top ten ranked pathways with high relevance to NP and neuroinflammation are presented in Fig. 3E. Moreover, the TNF pathway and neurotrophin signaling pathway were the top two key pathway. Critically, the enrichment of the neurotrophin signaling pathway provides the most direct network pharmacology evidence linking BBB to the BDNF-TrkB axis. This KEGG pathway explicitly encompasses BDNF binding to TrkB receptors and the activation of core downstream targets identified in our PPI network, solidifying the connection between BBB's predicted targets and the BDNF-TrkB signaling cascade central to NP pathophysiology.

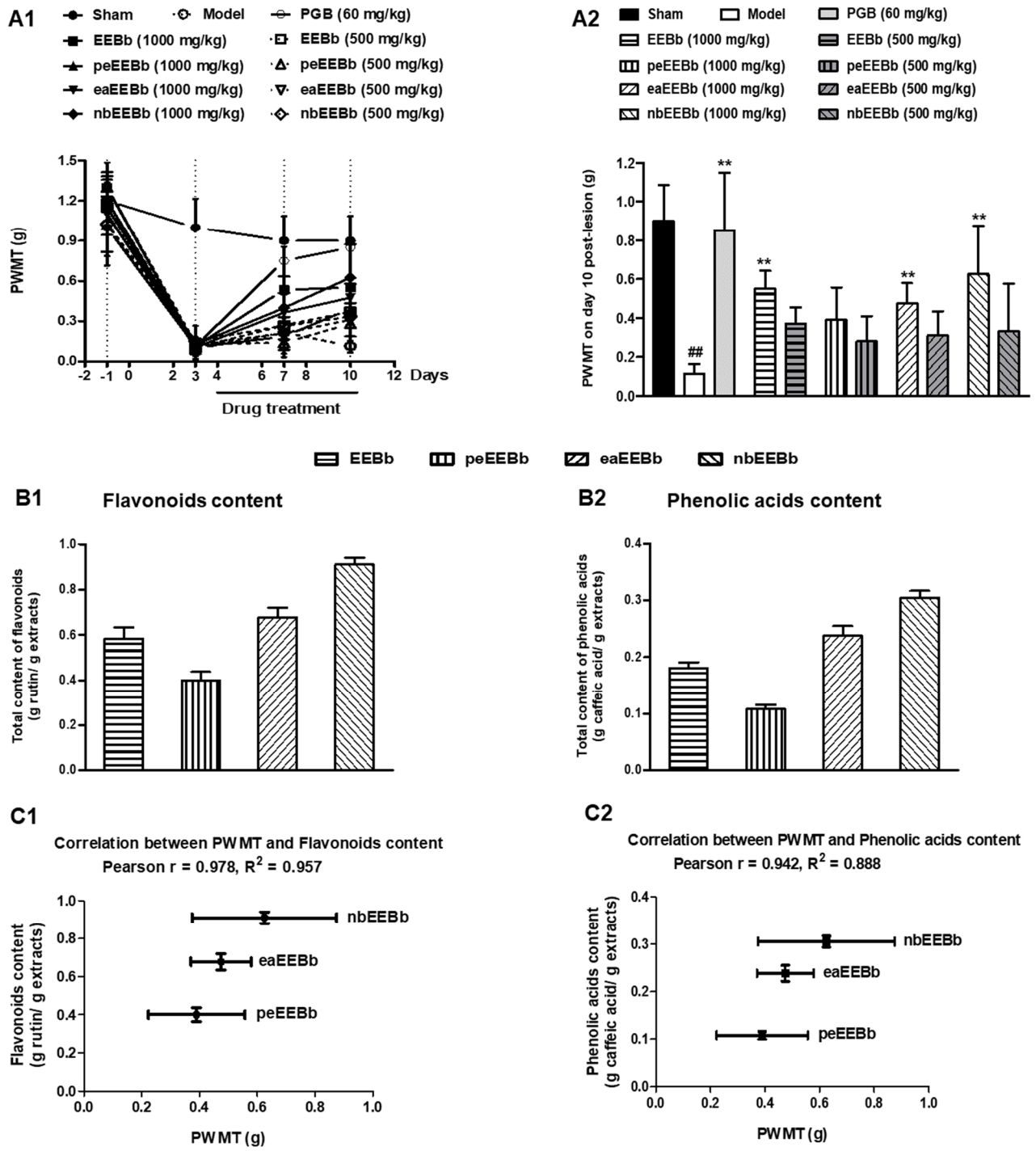

Fig. 1: Graph A showing the value change of PWMT (A1) in mice throughout the experiment, and the PWMT value on the 10th day after PSNL (A2). "Day 0" indicates the day of surgery. Graph B showing the determination of the total content of flavonoids (B1) and phenolic acids (B2) in different soluble extract fractions from EEBb by the colorimetric method. Graph C showing the correlations between PWMT on the 10th day after PSNL in different soluble extract fractions from EEBb (1000 mg/kg) and different active substances (flavonoids, C1, and phenolic acids, C2). PGB, pregabalin. Each group consists of 8 (graph A) or 6 (graph B) data. Data are shown as mean ± SD. $^{\#\#}P < 0.01$ compared to the sham group. $^{**}P < 0.01$ compared to the model group.

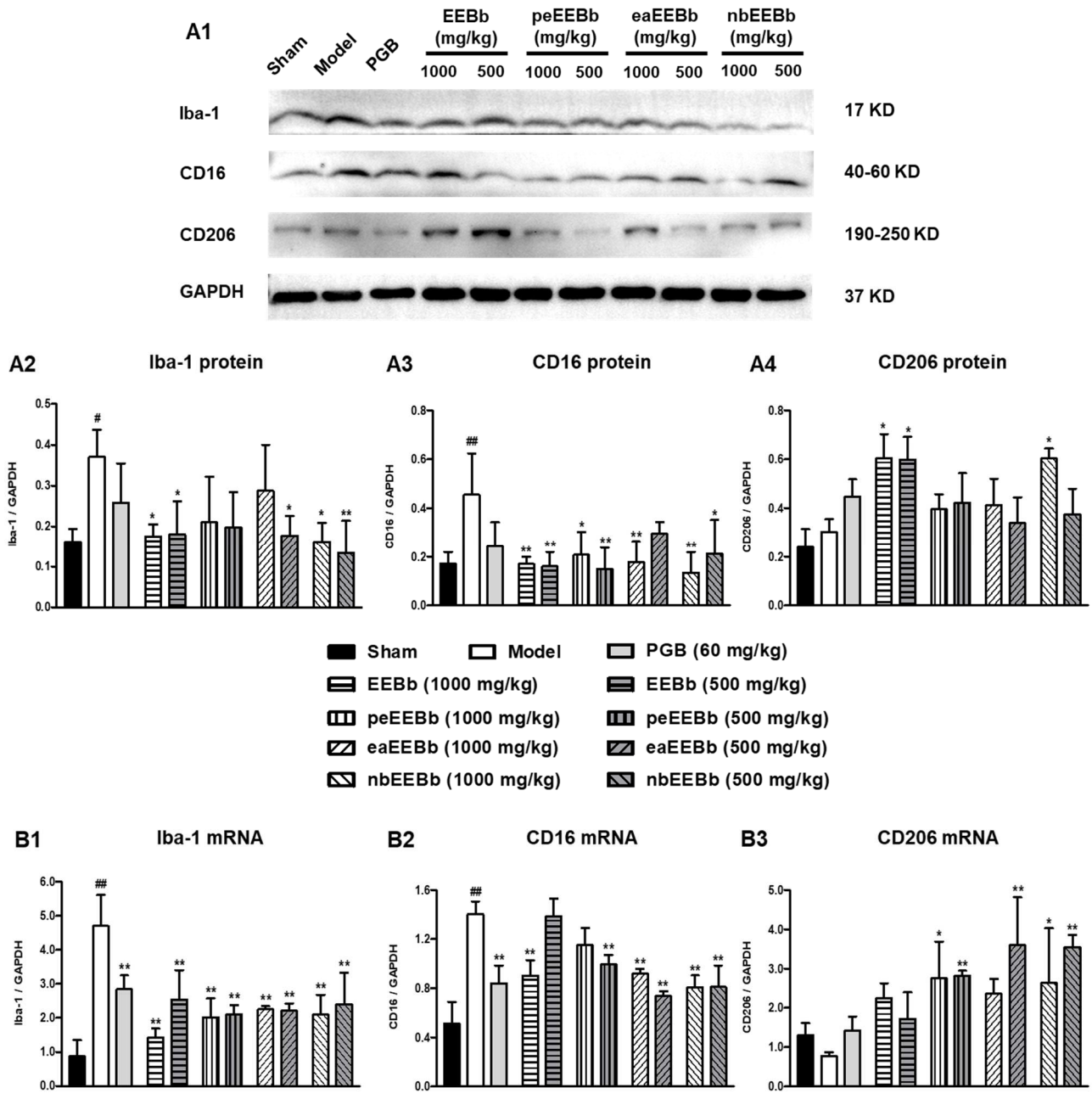

Fig. 2: Graph A showing the expressions of different subtype microglia in protein level by western blot analysis. A1 was the western blot results. A2-A4 were the statistical analysis of protein expressions. Graph B showing the expressions of different microglia subtype in gene level by qRT-PCR analysis. B1-B3 were the statistical analysis of gene expressions. The total, M1 subtype, and M2 subtype microglia in the spinal cord tissue (L4-L6), was marked by Iba-1, CD16, and CD206, respectively. PGB, pregabalin. Each group consists of 4 data. Data are shown as mean ± SD. $^{\#}P < 0.05$, $^{\#\#}P < 0.01$ compared to the sham group. $^{*}P < 0.05$, $^{**}P < 0.01$ compared to the model group. Significant difference was determined by the one-way ANOVA followed by the Tukey´s test.

nbEEBb inhibits P2X4R-BDNF-TrkB pathway in vivo and in vitro

Based on network pharmacology prediction, an important neurotrophin signaling pathways "P2X4R-BDNF-TrkB", which connects overactivated microglia and sensitized neuron, was selected for verification of the BBB acting mechanism on NP. 1000 mg/kg nbEEBb was used as objective due to its great effect on mechanical hyperalgesia and microglia' function of PSNL mice.

In vivo, nbEEBb produced a significant increase of PWMT in PSNL mice, but had no effect on normal mice (Fig. 4A).

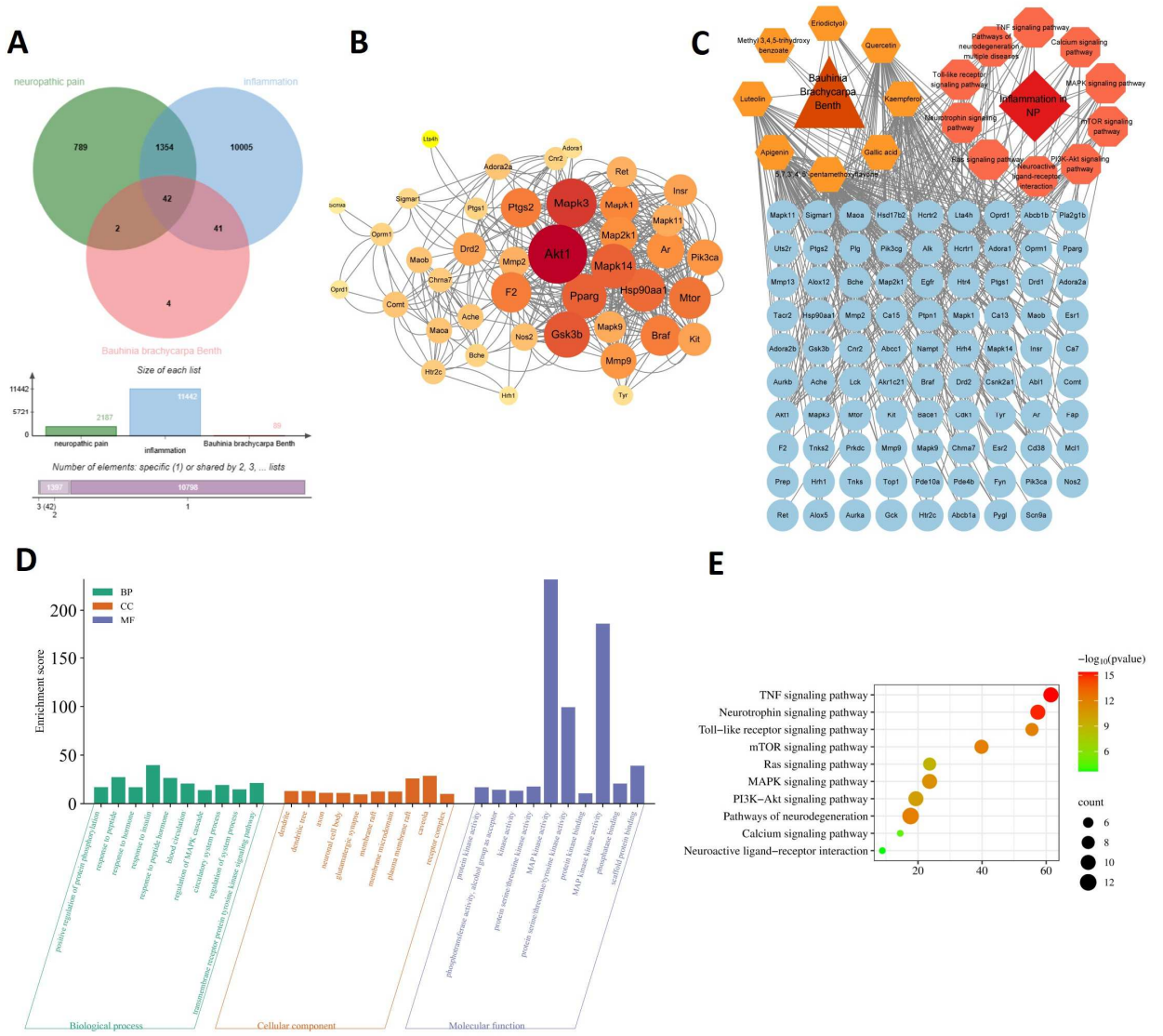

Fig. 3: Graph A is Venn diagram of overlapping genes associated with NP-related inflammation in BBB. Graph B showing the protein-protein network of the compound-disease target interactions. Graph C showing the compound-target-disease network of BBB in the treatment of NP-related inflammation. Graph D is the top 10 results from GO enrichment analysis. BP, biological processes. CC, cell compositions. MF, molecular functions. Graph E is the top 10 results from KEGG enrichment analysis.

In protein level, western blot results obtained from lumbar tissue showed that, compared to normal control, nbEEBb had no obvious effects on most protein expressions of P2X4R-BDNF-TrkB pathway ($P > 0.05$), except for the decrease of P2X4R and p38 ($P < 0.01$) and the increase of BDNF ($P < 0.05$) (Fig. 4B). However, all protein expressions of the pathway were activated after PSNL and nbEEBb had the ability of downregulating the expressions of P2X4R, BDNF, p-p38, the ratio of p-p38/p38, Trk B and p-Trk B ($P < 0.01$ or $P < 0.05$, Fig. 4B). In mRNA level, compared to normal control, it is surprisingly that the effects of nbEEBb on mRNA expressions were different with which of protein expressions. nbEEBb significantly suppressed the mRNA expressions of P2X4R and BDNF, while remarkably upregulated Trk B mRNA expression (Fig. 4C). After PNSL, the influences of nbEEBb on the mRNA expressions of components in P2X4R-BDNF-TrkB signal pathway were similar as protein levels. nbEEBb significantly depressed mRNA overexpression of P2X4R, BDNF and Trk B ($P < 0.01$ compared to PNSL model, Fig 4C) as well as the secretion of serum BDNF in PSNL mice (Fig 4D). *In vitro*, a model of BDNF over release that induced by ATP (the natural neurotransmitter of P2X4R) was established in BV2 microglia. Firstly, after pre-experiment, we chose 1 h treatment of 50 μM ATP as the model establish condition and 12 h incubation of 0.3 mg/ml nbEEBb as drug treatment condition, because these conditions induced obvious change of intracellular BDNF mRNA level without obvious impact on cell viability. Then, the effects of nbEEBb on P2X4R-BDNF pathway in BV2

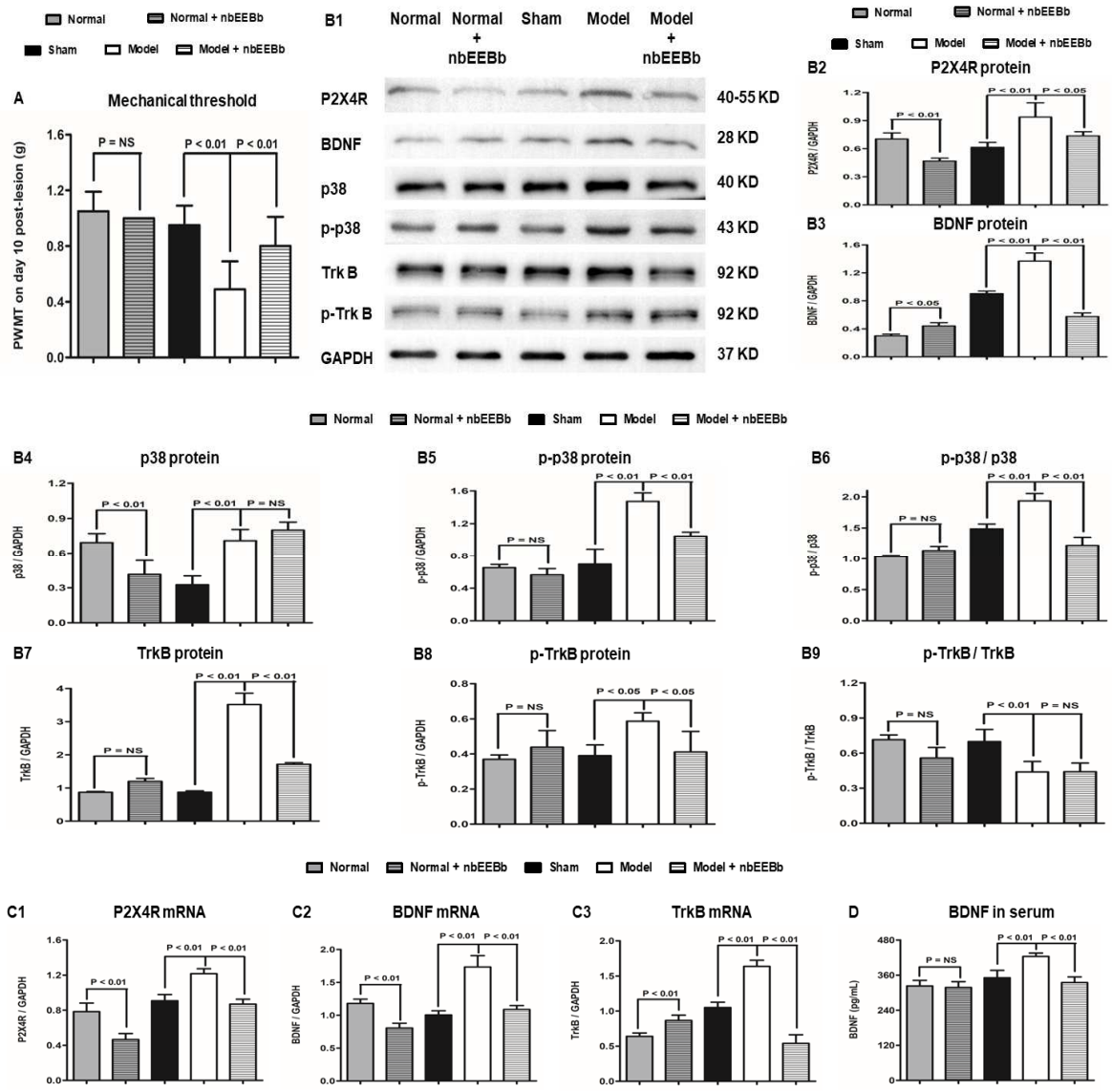

Fig. 4: Graph A showing the PWMT on the 10th day after PSNL. Graph B showing the protein expressions of "P2X4R-BDNF-TrkB" pathway *in vivo* by western blot analysis. B1 was the western blot results. B2-B9 were the statistical analysis of protein expressions. Graph C showing the gene expressions of the pathway *in vivo* by qRT-PCR analysis. C1-C3 were the statistical analysis of gene expressions. Graph D showing the content of BDNF in serum. Each group consists of 8 (graph A and D) or 4 (graph B and C) data. Data are shown as mean ± SD.

were studied formally. The results of western blot showed nbEEBb took little action on normal protein levels of intracellular P2X4R, BDNF, p-p38 and the ratio of p-p38/p38 ($P > 0.05$ compared to normal control, Fig 5A), except for the inhibition of p38 ($P < 0.05$). After ATP stimulation, all protein expressions in P2X4R-BDNF pathway were sharply escalated and nbEEBb significantly downregulated the expressions of P2X4R, BDNF, p38, p-p38 and the ratio of p-p38/p38 ($P < 0.01$compared to model, Fig. 5A). The results of PCR were consistent with that of western blot, that is, nbEEBb still had no obvious effects on normal intracellular mRNA expressions of P2X4R and BDNF as well as the normal supernatant content of BDNF ($P > 0.05$ compared to normal control, Fig. 5B).

However, the treatment of nbEEBb on BV2 markedly depressed mRNA overexpression of P2X4R and BDNF induced by ATP ($P < 0.01$compared to model, Fig. 5B) as well as BDNF release after ATP stimulation ($P < 0.01$, Fig. 5C).

DISCUSSION

The pantropical and subtropical genus *Bauhinia* has been used in folk medicine since ancient times to treat various diseases, especially inflammation-related disorders (Jiang B and Xiao CJ, 2021). Recent research in pantropical countries, particularly India and Brazil, have demonstrated that several *Bauhinia* species and their bioactive

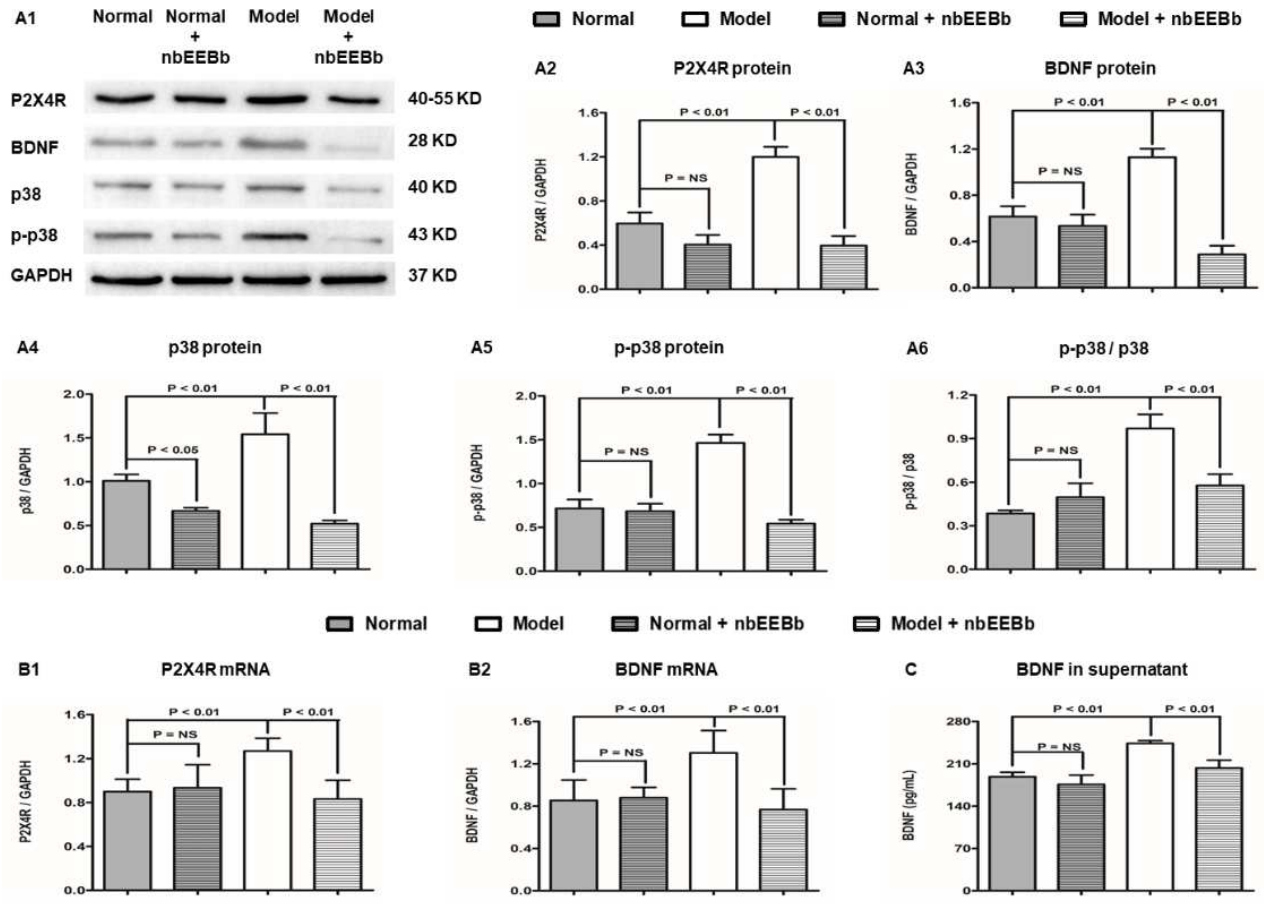

Fig. 5: Graph A showing the protein expressions of "P2X4R-BDNF" pathway *in vitro* by western blot analysis. A1 was the western blot results. A2-A6 were the statistical analysis of protein expressions. Graph B showing the gene expressions of the pathway *in vitro* by qRT-PCR analysis. B1-B2 were the statistical analysis of gene expressions. Graph C showing the content of BDNF in supernatant of medium. Each group consists of 4 (graph A and B) or 6 (graph C) data. Data are shown as mean ± SD.

constituents exhibit antinociceptive effects consistent with traditional uses (Mohamed MA *et al*., 2010; Pinto IR *et al*., 2020). Unlike previous studies that predominantly relied on crude extracts, we employed systematic fractionation of BBB to trace the active ingredients and then acquired the most effective fraction for alleviating mechanical hyperalgesia in NP, that is the nbEEBb. The antinociceptive effect of BBB may be attributable to their bioactive constituents. Existing studies report that *Bauhinia* species predominantly contain terpenes, steroids, alkaloids, saponins and notably flavonoids (Islam MM *et al*., 2022; Wu XD *et al*., 2020). Recently, UPLC-Triple TOF mass spectrometry has been employed to analyze the chemical composition of nbEEBb. Preliminary analysis indicated the chemicals in nbEEBb including alkaloids, sugars, glycosides, nucleosides and nucleotides, organic acids, flavonoids and their derivatives. These data are currently being processed and remain unpublished. Conventional analytical methods in this study further confirmed that nbEEBb is rich in flavonoids and phenolic acids. Numerous studies have reported that flavonoids and phenolic acids isolated from other plants can effectively treat NP (Vyas A *et al*., 2024; Gu J *et al*., 2025). Our results also indicated that the antinociceptive effect of different fractions from EEBb positively correlates with total flavonoid and phenolic acid contents in them. However, Further investigation is required to determine whether the antinociceptive efficacy of BBB arises from synergistic interactions among multiple components or arises from individual substances. Advances in neurobiology and deeper understanding of NP mechanisms have facilitated multitarget therapy development. Up to now, traditional treatments for NP still focused on abnormal neuronal action potentials caused by ion channel dysfunction. But central and peripheral sensitization driven by inflammatory mediator accumulation from non-neural cells at injury sites become another attractive target of the treatment of NP recently (Saunders MN *et al*., 2023). Microglia is the key mediator of central sensitization in NP (Li XL *et al*., 2021; Wang LJ *et al*., 2020). In response to various stimuli, microglia rapidly adapt to their environment, polarizing into two distinct activation states: M1 macrophages (pro-

inflammatory) that exacerbate NP and M2 macrophages (anti-inflammatory) that alleviate NP (Atta AA *et al*., 2023; Lu X *et al*., 2023). Activated microglia subsequently produce inflammatory mediators that induce neuronal hyperexcitation and central sensitization (Karavis MY *et al*., 2023). Therefore, the effects of EEBb and its fractions on regulation of microglia were evaluated both in protein and mRNA levels in our study. The findings revealed that nbEEBb exhibited the strongest potential to suppress total microglial activation labeled with Iba-1, significantly reduced the pro-inflammatory M1 subtype labeled with CD16 and effectively enhanced the anti-inflammatory M2 subtype labeled with CD206. Moreover, above effects of nbEEBb were related to the dose, in detail, 500 mg/kg nbEEBb had more powerful ability of inhibiting Iba-1 protein expression and enhancing CD206 mRNA expression, while 1000 mg/kg nbEEBb showed more stronger power of downregulating CD16 protein level and upregulating CD206 protein level. EEBb and other fractions also had the dose-dependent actions, for example, 1000 mg/kg EEBb had the better ability of inhibiting the mRNA expression of Iba-1 and CD16 than 500 mg/kg EEBb and both two doses of EEBb had similar intensity of regulating the protein levels of Iba-1, CD16 and CD206. peEEBb had obvious effects on CD16 protein expression and the mRNA expression of Iba-1, CD16 and CD206 and 500 mg/kg peEEBb had more efficacious or similar action than 1000 mg/kg peEEBb. 1000 mg/kg eaEEBb was good at depressing CD16 protein level than 500 mg/kg eaEEBb, while 500 mg/kg eaEEBb had better performance of regulating Iba-1 protein level and the mRNA levels of CD16 and CD206. This observed dose-dependent variability in EEBb fractions' effects on microglial markers aligns with reports on other modulators. For instance, scriptaid (a histone deacetylase inhibitor) effectively promotes M2 polarization at 1 μmol/L but loses efficacy and causes cytotoxicity at ≥ 2 μmol/L, illustrating a narrow optimal window (Guo QX *et al*., 2024). Similarly, sodium butyrate suppresses M1 markers at both 0.125 mmol/L and 0.25 mmol/L, but the higher dose induces significantly greater reductions in NO and TNF-α, suggesting dose-dependent pathway engagement (Wang LJ *et al*., 2023). Plant extracts like kaempferol and DHA also exhibit distinct dose-response patterns for specific microglial targets (Zhong Y and Shan R, 2023). Thus, the differential impact of low versus high doses of nbEEBb, peEEBb and eaEEBb on Iba-1, CD16 and CD206 expression reflects a common phenomenon where optimal microglial modulation is compound-specific and may preferentially target M1 suppression or M2 promotion at different concentrations. However, the mechanism of effect difference caused by dose was unclear in this study and need to further studied.

For deep investigation of BBB acting mechanism on NP, network pharmacology was applied firstly for prediction. The findings indicated that BBB's antinociceptive effects engage several inflammatory pathways, particularly the neurotrophin signaling pathway. We prioritized the P2X4R-BDNF-TrkB signaling pathway given its crucial role mediated neuron-microglia interaction in NP. P2X4R, an ATP-gated cation channel, is exclusively upregulated in spinal microglia after injury. Evidence from studies demonstrates that blocking P2X4R alleviates allodynia and its knockout in mice confers resistance to NP, highlighting its critical function in NP pathology. (Inoue K *et al*., 2018). Microglial P2X4R activation triggers the release of BDNF, which is a key mediator for central sensitization. (Long T *et al*., 2020; Inoue K *et al*., 2018). After that, BDNF binds to and activates the neuronal TrkB receptor, initiating downstream signaling pathways including PI3K/Akt, MAPK/ERK and PLC-γ. These signal cascades lead to hyperexcitability by enhancing excitatory NMDA function and downregulating inhibitory GABAergic function (Inoue K *et al*., 2018; Chenguang X *et al*., 2018; Long T *et al*., 2020; Loggia ML *et al*., 2024; Huang RY *et al*., 2023). Subsequent studies were carried out *in vivo* and *in vitro* to confirm the proposed mechanism. The findings indicated that nbEEBb exerted no significant effect on the normal expression levels of key protein components in the P2X4R-BDNF-TrkB pathway but markedly inhibited their upregulation at various molecular levels upon stimulation by nerve ligation or receptor activation. *In vivo*, aside from impacting P2X4R, BDNF and p38, nbEEBb had minimal effect on normal protein expressions across most components of the pathway, especially the ratios of p-p38 / p38 and p-TrkB / TrkB, which represent protein activation states. The conclusion was further confirmed *in vitro* that nbEEBb rarely changed the normal protein and gene expressions of P2X4R-BDNF pathway components in BV2 cells. The discrepancy in nbEEBb's effects observed between mice and isolated cells likely due to the more complex inflammatory regulatory networks *in vivo*. After the activation of all the signal molecules in P2X4R-BDNF-TrkB pathway by nerve injury *in vivo* or ATP stimulation *in vitro*, nbEEBb displayed strong powers to inhibit nearly all the expressions of these signal molecules both in protein and gene levels, except for little effect on p38 protein and p-TrkB / TrkB *in vitro*. The reason for inaction of nbEEBb on p-TrkB / TrkB is account for the stronger ability of nbEEBb on TrkB than on p-TrkB. Overall, the depression of nbEEBb on activated state of P2X4R-BDNF-TrkB signaling pathway is far beyond its influence on normal state of this pathway. In summary, this study demonstrated that nbEEBb exhibited superior antinociceptive efficacy against NP, primarily through inhibiting the microglia-mediated P2X4R-BDNF-TrkB signaling pathway, which links glial activation to neuronal sensitization. Notably, nbEEBb preferentially suppresses the activated state of this pathway (both *in vivo* and *in vitro*) with minimal impact on baseline activity. The findings suggested that nbEEBb could influence modulation of injury-induced plasticity. However, certain limitations remain in our study. Although chemical profiling identified flavonoids/phenolic acids as candidate active constituents, the definitive identification

of specific compounds in plant extracts remains necessary. Additionally, while the optimal dose was employed in the mechanism study, multi-dose validation was not conducted. Furthermore, the effects of BBB extractions on microglia polarization should be verified by colocalization of Iba-1 and CD16 or Iba-1 and CD206 to avoid result deviation caused by nonspecific markers. All these limitations should be offset in future work.

CONCLUSION

In conclusion, EEBb and the different portions partitioned from EEBb alleviated mechanical hyperalgesia in NP, and their antinociceptive effects are correlated to the content of flavonoids and phenolic acids. M1/M2 microglia/macrophage polarization is involved in their antinociceptive effects. nbEEBb has stronger or at least similar ability to EEBb in the regulation of microglia/macrophage polarization, and could be an option for the treatment of NP.

Acknowledgments
The authors gratefully acknowledge the financial support from the Research Programs of Yunnan Education Department and the Special Basic Cooperative Research Programs of Yunnan Provincial Undergraduate Universities Association. We also extend our thanks to the technical staff at our institution for their assistance in animal care and experimental procedures.

Author's contributions
Han-Fu Liu performed research and wrote the paper. Ya-Nan Chen performed research. He Sun analyzed data. Bei Jiang offered help with the chemistry experiment. Jin-Da Wang provided the idea of the study and designed research. Lei Shen provided the idea of the study, designed research and revised the manuscript.

Funding
This work was financially supported by the Research Programs of Yunnan Education Department (No. 2024J0838) and the Special Basic Cooperative Research Programs of Yunnan Provincial Undergraduate Universities' Association (No. 2018FH001-096).

Data availability statement
All data generated or used during the study appear in the submitted article.

Ethical approval
All animal-related experimental procedures adhered to the ethical principles and regulatory guidelines of the Declaration of Helsinki Chinese Society of Laboratory Animals and were approved by the Experimental Animal Ethics Committee of Dali University (Approval number: No. 2021-p2-093).

Conflicts of interest
The authors declare that they have no conflicts of interest.

Supplementary data
https://www.pjps.pk/uploads/2026/02/SUP1770031447.pdf

REFERENCES

Atta AA, Ibrahim WW, Mohamed AF and Abdelkader NF (2023). Microglia polarization in nociplastic pain: Mechanisms and perspectives. *Inflammopharmacology*, **31**(3): 1053-1067.

Bannister K, Sachau J, Baron R and Dickenson AH (2020). Neuropathic pain: Mechanism-based therapeutics. *Annu. Rev. Pharmacol. Toxicol*., **60**: 257-274.

Chen YN, Liu HF, Sun H, Xiao CJ, Jiang B and Shen L (2022). Antinociceptive effect of ethanolic extract of *Bauhinia brachycarpa* Benth on neuropathic pain model induced by partial sciatic nerve ligation. *J. Ethnopharmacol*., **295**: 115412.

Chen YN, Liu HF, Xiao CJ, Jiang B and Shen L (2022). Effects of *Bauhinia brachycarpa* Benth on neuropathic pain model rats. *Chin. Tradit. Patent Med*., **44**(6): 1970-1973.

Chenguang X, Van Sy M, Ran X, Eyad HA and Usman AK (2018). Linear Convergence in Optimization over Directed graphs with row-Stochastic matrices. *IEEE Trans. Autom. Control*, **63**(10): 3558-3565.

Chuxiong Institute for drug control (1983). Yi Medicine Records, 1st ed. Sichuan Ethnic Press, Chengdu, pp. 116-117.

Colloca L, Ludman T, Bouhassira D, Baron R, Dickenson AH, Yarnitsky D, Freeman R, Truini A, Attal N, Finnerup NB, Eccleston C, Kalso E, Bennett DL, Dworkin RH and Raja SN (2017). Neuropathic pain. *Nat. Rev. Dis. Prim*., **3**: 17002.

Davis M, Borucki B, Rohrer B and Tomlinson S (2024). Complement propagates visual system pathology following traumatic brain injury. *J. Neuroinflammation*, **21**: 0.

Echeverria VM, Tortorici V, Brito BE, Ryskamp D, Uribe A and Weaver T (2024). The role of neuroinflammation in the transition of acute to chronic pain and the opioid-induced hyperalgesia and tolerance. *Front. Pharmacol*., **14**: 1297931.

Editorial Committee of the Flora of China of Chinese Academy of Science (1980). Flora of China. Science Press, Beijing, pp. 160.

Gard A, Vedung F, Piehl F, Khademi M, Wernersson MP, Rorsman I, Tegner Y, Pessah-Rasmussen H, Ruscher K and Marklund N. (2023). Cerebrospinal fluid levels of neuroinflammatory biomarkers are increased in athletes with persistent post-concussive symptoms following sports-related concussion. *J. Neuroinflammation*, **20**: 0.

Gong M, Lu J and Xiao Y (2019). Determination of total flavonoids and three main aglycones in *Artemisiae argyi folium* from different habitats. *China Pharm*., **22**(5): 966-968,975.

Gu J, Wang J, Fan H, Wei Y; Li Y, Ma C, Xing K, Wang P, Wu Z, Wu T, Li X, Zhang L, Han Y, Chen T, Qu J, Yan

X. (2025). Decoding the mechanism of proanthocyanidins in central analgesia: Redox regulation and KCNK3 blockade. *Exp. Mol. Med*., **57**: 0.

Guo QX, Wang Y and Wu T (2024). Scriptaid-loaded methacrylated silk fibroin hydrogel regulates microglial polarization behavior. *Chin. J. Tissue Eng. Res*, **28**(29): 4628-4633.

Hu NH, Liu J, Luo Y, Li YX. (2024). A comprehensive review of traditional Chinese medicine in treating neuropathic pain. *Heliyon*, **10**(17): e37350

Huang RY, Song YF, Zhou M, Xu HM, Liu J, Zhang MM, Gao Y and Xiong W (2023). Experimental study on trigeminal neuralgia mediated by overexpression of P2X4 receptor. *Chin. J. Pain Med*., **30**(5): 123-128.

Inoue K and Tsuda M (2018). Microglia in neuropathic pain: Cellular and molecular mechanisms and therapeutic potential. *Nat. Rev. Neurosci*., **19**(3): 138-152.

Islam MM, Alam R, Chung HJ, Emon NU, Kabir MF, Rudra S, Alam S, Ullah A, Hong ST and Sayeed MA (2022). Chemical, pharmacological and computerized molecular analysis of stem's extracts of *Bauhinia scandens* L. provide insights into the management of diarrheal and microbial infections. *Nutrients*, **14**(2): 265.

Jiang B and Xiao CJ (2021). Modern Research and Application of Bai Characteristic Medicinal Plants. China Press of Traditional Chinese Medicine, Beijing.

Karavis MY, Siafaka I, Vadalouca A and Georgoudiset G (2023). Role of microglia in neuropathic pain. *Cureus*, **15**(8): e43555.

Karavis MY, Siafaka I, Vadalouca A and Georgoudiset G (2023). Role of microglia in neuropathic pain. *Cureus*, **15**(8): e43555.

Kaye AD, Armistead G, Amedio LS, Manthei ME, Ahmadzadeh S, Bernhardt B, Shekoohi S. (2025). Evolving treatment strategies for neuropathic pain: A narrative review. *Medicina (Kaunas)*, **61**(6): 1063.

Li SH, Li L, Yang RN and Liang SD (2020). Compounds of traditional Chinese medicine and neuropathic pain. *Chin. J. Nat. Med*., **18**(1): 28-35.

Li XL, Guo QL, Ye Z, Wang E, Zou WY, Sun ZH, He ZH, Zhong T, Weng YQ and Pan YD (2021). PPAR γ prevents neuropathic pain by down-regulating CX3CR1 and attenuating M1 activation of microglia in the spinal cord of rats using a sciatic chronic constriction injury model. *Front. Neurosci*., **15**: 620525.

Loggia ML (2024). "Neuroinflammation": does it have a role in chronic pain? Evidence from human imaging. *Pain*, **165**: 0.

Long T, He W, Pan Q, Zhang S, Zhang D, Qin G, Chen L, Zhou J. (2020). Microglia P2X4R-BDNF signalling contributes to central sensitization in a recurrent nitroglycerin-induced chronic migraine model. *J. Headache Pain*, **21**(1): 4.

Lu X, Chen LH, Jiang C, Cao KL, Gao ZH and Wang Y (2022). Microglia and macrophages contribute to the development and maintenance of sciatica in lumbar disc herniation. *Pain*, **164**(2): 362-374.

Mohamed MA, Mammoud MR and Hayen H (2010). Evaluation of antinociceptive and anti-inflammatory activities of a new triterpene saponin from Bauhinia variegata leaves. *Z. Naturforsch. C. J. Biosci*., **64**: 798-808.

Pinto IR, Chaves HV, Freire JMO, Sousa LHT, Monteiro DAM, Costa JJN, Pereira KMA, Santiago GMP, Sousa LM, Silva MR, Monteiro AD, Montenegro RC, Moraes MEA, Filho GC, Pinto VPT and Bezerra MM (2020). A semi-synthetic flavonoid from *Bauhinia pulchella* stem attenuates inflammatory osteolysis in periodontitis in rats: Impact on cytokine levels, oxidative stress and RANK/RANKL/OPG pathway. *Arch. Oral. Biol.*, **117**: 104816.

Saunders MN, Griffin KV, Kalashnikova I, Kolpek D, Smith DR, Saito E, Cummings BJ anderson AJ, Shea LD and Park J (2023). Biodegradable nanoparticles targeting circulating immune cells reduce central and peripheral sensitization to alleviate neuropathic pain following spinal cord injury. *Pain*, **165**(1): 37463227.

Shan H (2017). Anti-nociceptive activity screening of the Plants from West Yunnan and analgesic activity of Bauhinia Brachycarpa [Master's thesis]. Dali University.

Sun C, Deng JH, Ma YF, Meng FQ, Gui X, Li M, Li JT, Li J, Yin PB, Kong LJ, Zhang LC and Tang PF (2023). The dual role of microglia in neuropathic pain after spinal cord injury: Detrimental and protective effects. *Exp. Neurol*., **370**: 114570.

Vyas A, Gupta R and Jatav R (2024). *In-vitro* antioxidant and *in-vivo* analgesics and anti-inflammatory activity of allamanda blanchetii leaf extract in rats. *Antiinflamm Antiallergy Agents Med Chem*, undefined: 0.

Wang LJ, Yin C, Liu TY, Abdul M, Zhou Y, Cao JL and Lu C (2020). Pellino1 regulates neuropathic pain as well as microglial activation through the regulation of MAPK/NF-κB signaling in the spinal cord. *J. Neuroinflammation*, **17**: 83.

Wang LJ, Zhang AR, Zhang X, Liu JC, Yang Y, Pang RC, Hu YH. (2023). Sodium butyrate regulates LPS-induced BV2 microglial phenotypic polarization via TLR4/NF-κB signaling pathway. *J. Army Med. Univ*, **45**(17): 1846-1853.

Wu XD, Xie JZ, Qiu L, Zou LH, Huang YF, Xie YF, Xu HJ, He SN and Zhang Q (2020). The anti-inflammatory and analgesic activities of the ethyl acetate extract of Viburnum taitoense Hayata. *J. Ethnopharmacol*., **269**: 113742.

Zhang Y, Yu ZY, Geng FN, Wu TQ, Yang L, Xiao H, Zhao Y and Liu H. (2018). Optimization of determination method for total phenolic acids in dandelion extract. *Food. Res. Dev*., **39**(3): 123-126.

Zhong Y and Shan RA (2024). Research progress on microglial polarization in chronic pain. *J. Clin. Anesthesiol*, **40**(02): 200-203.